

## 11 Lattice gauge models: a brief introduction

### 11.1 INTRODUCTION: GAUGE INVARIANCE AND LATTICE GAUGE THEORY

Lattice gauge theories have played an important role in the theoretical description of phenomena in particle physics, and Monte Carlo methods have proven to be very effective in their study. In the lattice gauge approach a field theory is defined on a lattice by replacing partial derivatives in the Lagrangian by finite difference operators. For physical systems a quantum field theory on a four-dimensional space-time lattice is used, but simpler models in lower dimension have also been studied in hope of gaining some understanding of more complicated models as well as for the development of computational techniques.

We begin by describing the potential  $A_\mu^\alpha(x)$  in terms of the position  $x$  in space-time. The rotation  $U$  of the frame which relates neighboring space-time points  $x^\mu$  and  $x^\mu + dx^\mu$  is given by

$$U = \exp \{ i g A_\mu^\alpha(x) \lambda_\alpha dx^\mu \}, \quad (11.1)$$

where  $g$  is the coupling constant and the  $\lambda_\alpha$  are the infinitesimal generators of the gauge group. When the field is placed on a lattice, an element  $U_{ij}$  of the gauge group is assigned to each link between neighboring sites  $i$  and  $j$  of the lattice, subject to the condition that

$$U_{ij} \rightarrow U_{ij}^{-1}. \quad (11.2)$$

Gauge transformations are then defined by

$$U_{ji} \rightarrow U'_{ji} = g_i U_{ji} g_i^{-1} \quad (11.3)$$

where  $g_i$  is a group element. There will be some elementary closed path on the lattice which plays the role of the infinitesimal rectangular closed path which defines the transporter; for example, the path around an elementary square on a hypercubical lattice (or 'plaquette') is

$$U_p = U_{ij} U_{jk} U_{kl} U_{li}, \quad (11.4)$$

where the 'action' associated with a plaquette is

$$S_p = \beta f(U_p). \quad (11.5)$$

$f(U_P)$  is commonly referred to as the (internal) energy of the plaquette, and the choice

$$f(U_P) = 1 - \frac{1}{2} \text{Tr} U_P = 1 - \cos \theta_P \quad (11.6)$$

is termed the Wilson action, although many other forms for the action have been studied.

By first making a Wick rotation to imaginary time, we can define the observables in a Euclidean four-dimensional space, i.e.

$$\begin{aligned} \langle O \rangle &= \frac{1}{Z} \int \mathcal{D}A_\mu O(A_\mu) \exp[-S(A_\mu)] \\ &\rightarrow \frac{1}{Z} \sum_{\{U_{ij}\}} O(U_{ij}) \exp\{-S(U_{ij})\}, \end{aligned} \quad (11.7)$$

where

$$Z = \int dA \exp(-S(A)) \rightarrow \sum_{\{U_{ij}\}} \exp\{-S(U_{ij})\}, \quad (11.8)$$

where the sums are over the dynamic variables  $U_{ij}$ . Note that the above equations are equivalent, in a formal sense, to those which describe the behavior of an interacting particle system within the framework of statistical mechanics. In this view,  $\beta$  becomes equivalent to the inverse temperature and  $f(U_P)$  plays the role of the Hamiltonian. With the analogy to statistical mechanics, one can carry out Monte Carlo simulations by updating the link variables, e.g. using a Metropolis method, and then calculating expectation values of quantities of interest. Thus, all of the tools needed for the study of lattice gauge models are already in place. In order to recover a non-trivial continuum field theory, the lattice constant must be allowed to go to zero, but the product  $a\lambda(g)$  must remain constant. The critical point  $g_{\text{cr}}$  for which this occurs must then have scaling properties, and in the language of statistical mechanics this means that a phase transition must occur. For any ‘interesting’ behavior to remain, this means that the equivalent of the correlation length must diverge, i.e. a second order phase transition appears. Thus, one important goal is to determine the phase diagram of the theory. As a consequence, many of the methods of analysis of the Monte Carlo data are identical to those of the systems discussed in earlier chapters, although the interpretation of the various quantities is completely different.

Note that the same problems with finite size effects, boundary conditions, etc. that we encountered in Chapters 4 and 5 in the study of spin systems apply here, and we refer the reader back to these earlier chapters for a detailed discussion. Indeed, the problems are even more severe for the four-dimensional lattice gauge theories of real interest since there is a much higher percentage of ‘spins’ on the boundary than for lower dimensional magnetic systems. Furthermore, the determination of new link values may be very complicated, particularly for groups such as  $\text{SU}(2)$  and  $\text{SU}(3)$ , so special sampling methods have been devised.

## 11.2 SOME TECHNICAL MATTERS

Various specialized techniques have been devised to try to make Monte Carlo sampling more efficient for lattice gauge theories. The special problem which one encounters in lattice gauge studies is that the determination of the new configuration and its energy are often extremely time consuming. As a result the 'standard' importance sampling methods often become inefficient. Among the techniques that are used are:

- (1) The heatbath method. Here a new link  $U'_{ji}$  is chosen with probability  $\exp\{-S(U'_{ji})\}$  regardless of the previous value of the link.
- (2) Multihit methods. Here the Metropolis algorithm is used, but the entire process is repeated on a single link  $n$  times before another link is chosen for consideration. This is efficient because the complexity of the interaction makes the computation of the possible new states considerably more complex than for spin models.
- (3) Mixed initial states. To overcome problems with metastability, one can begin with a state in which half of the system is in a 'cold' state and half in a disordered state. The time development is followed for different values of  $\beta$  to see towards which state the entire system evolves.

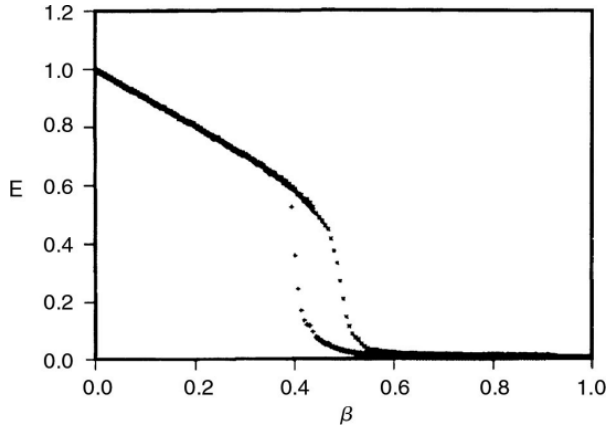
Another simplification which has also been used is to use a discrete subgroup as an approximation to the full group; in such cases the computation of the action is simplified although the model is obviously being modified and the consequences of these changes must be carefully examined.

## 11.3 RESULTS FOR $Z(N)$ LATTICE GAUGE MODELS

Perhaps the simplest lattice gauge theories are those in which the variables of interest are 'spins' which assume a finite number  $N$  of values distributed on a unit circle. While such models are not expected to be relevant to the description of physical systems, they play a useful role in the study of the phase structure of lattice gauge models since their relative simplicity allows them to be simulated rather straightforwardly. For the discrete  $Z(N)$  group the special case of  $N = 2$  corresponds to a gauge invariant version of the Ising model. (The  $U(1)$  theory, which will be discussed in the next section, corresponds to the  $N = \infty$  limit of  $Z(N)$ .) Creutz *et al.* (1979) examined the four-dimensional  $Z(2)$  gauge model and found evidence for a first order transition. In particular, sweeps in  $\beta$  exhibit strong hysteresis, and starts from either ordered or disordered states at the transition coupling show very different metastable states (see Fig. 11.1).

The critical behavior for the  $(2 + 1)$ -dimensional  $Z(2)$  lattice gauge model at finite temperatures (Wansleben and Zittartz, 1987) was calculated by looking at the block size dependence of the fourth order cumulant.  $128 \times 128 \times N_T$  lattices were examined where the number of lattice points in the temperature

Fig. 11.1 The average energy per plaquette as a function of  $\beta$  for the four-dimensional  $Z(2)$  lattice gauge theory. A hypercubic lattice with  $L_x = L_y = L_z = 8$  and  $L_t = 20$  with periodic boundary conditions was used. The ‘temperature’ was swept up and then back down. From Creutz *et al.* (1979).



direction,  $N_T$ , was varied. The value of  $\nu$  is apparently unity, but the estimate for  $\beta/\nu$  depended on  $N_T$ .

**Problem 11.1** Write a Monte Carlo program for the  $Z(2)$  lattice gauge model in four dimensions. Determine the behavior of the energy as a function of  $\beta$  for  $L = 3$ . Estimate the value of  $\beta$  at which the transition occurs. Compare your results with the data given in Fig. 11.1 and comment.

## 11.4 COMPACT U(1) GAUGE THEORY

The U(1) model has also been extensively studied and is a prime example of the difficulties associated with obtaining clear answers for lattice gauge models. Initial Monte Carlo examinations of the simple action

$$S = - \sum_P [\beta \cos \theta_P] \quad (11.9a)$$

could not determine if the transition was first or second order. The reason for the uncertainty became clear when an adjoint coupling was added so that the total action became

$$S = - \sum_P [\beta \cos \theta_P + \gamma \cos (2\theta_P)], \quad (11.9b)$$

where  $\theta_P$  is the plaquette angle, i.e. the argument of the product of U(1) variables around a plaquette  $P$ . The phase diagram in this expanded parameter space then showed that the transition actually changed order for a value of the adjoint coupling  $\gamma$  which was close to zero, and crossover phenomena make the interpretation for the pure U(1) model problematic. The most detailed study of this model (Jersák *et al.*, 1996a, 1996b) simulated spherical lattices and used reweighting techniques together with finite size scaling to conclude that for  $\gamma \leq 0$  the transition is indeed second order and belongs to the universality

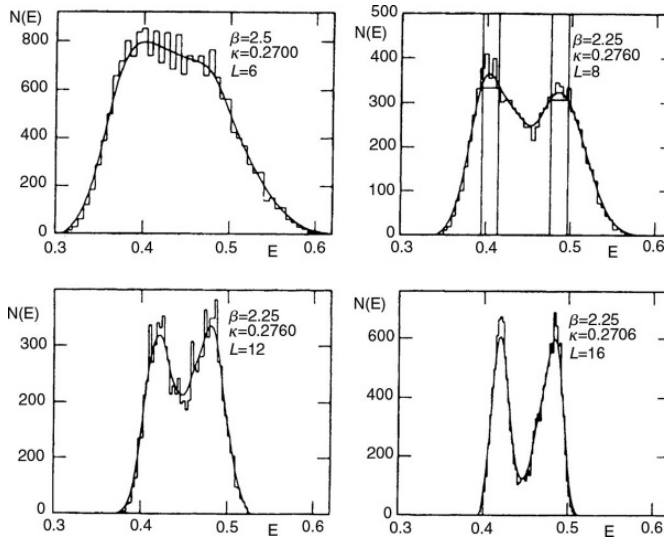


Fig. 11.2 A sequence of distribution functions  $N(E)$  near the transition at  $\beta = 2.25$  for different lattice sizes in the SU(2) model with Higgs fields. From Bock *et al.* (1990).

class of a non-Gaussian fixed point with the exponent  $\nu$  in the range 0.35–0.40 (the best estimate is  $\nu = 0.365(8)$ ).

**Problem 11.2** Perform a Monte Carlo simulation for the simple U(1) gauge model (i.e.  $\gamma = 0$ ) in four dimensions. Determine the variation of the energy as a function of  $\beta$  for  $L = 3$ . Estimate the location of the phase transition.

## 11.5 SU(2) LATTICE GAUGE THEORY

The transition between the weak coupling and strong coupling regimes for SU(2) lattice gauge theories at finite temperature has also been a topic of extensive study.

The Glashow–Weinberg–Salam (GWS) theory of electroweak interactions assumes the existence of a Higgs mechanism. This can be studied in the context of an SU(2) lattice gauge theory in which ‘spins’ are added to the lattice site and the Hamiltonian includes both gauge field and Higgs field variables:

$$S = -\frac{\beta}{4} \sum_P \text{Tr} (U_P + U_P^\dagger) - \kappa \sum_x \sum_{\mu=1}^4 \text{Re} (\text{Tr} \Phi_x^\dagger U_{x,\mu} \Phi_{x+\mu}) + \lambda \sum_x \frac{1}{2} \text{Tr} (\Phi_x^\dagger \Phi_x - 1)^2 + \sum_x \text{Tr} \Phi_x^\dagger \Phi_x. \quad (11.10)$$

For fixed  $\lambda$  there is a confinement region for  $\kappa < \kappa_c$  and a Higgs region for  $\kappa > \kappa_c$ . Even if  $\lambda$  is fixed at a physically reasonable value, the resultant phase diagram is in a two-dimensional parameter space and the nature of the transition appears to change order (Bock *et al.*, 1990). This can be seen in Fig. 11.2 where two equal peaks in the distribution develop with a very deep

well between them as the lattice size is increased. The use of histograms and finite size scaling aids in the analysis, but the location of a tricritical point was not possible with data for lattices up to  $16^4$  in size.

## 11.6 INTRODUCTION: QUANTUM CHROMODYNAMICS (QCD) AND PHASE TRANSITIONS OF NUCLEAR MATTER

According to our current understanding of high energy physics the basic constituents of elementary particles are quarks and gluons. Quantum chromodynamics (QCD) is the relativistically invariant quantum field theory, formulated in four-dimensional space ( $\mathbf{x}, \tau = it$ ); note that we choose here the standard units of elementary particle physics,  $\hbar = c = 1$ . Since for this problem of strong interactions perturbation theory is of limited value, non-perturbative theoretical approaches must be sought. A formulation in terms of path integrals is the method of choice (Creutz *et al.*, 1983; Kogut, 1983; Montvay and Münster, 1994). In this approach, the vacuum expectation value of a quantum observable  $\mathcal{O}$  is written as (Meyer-Ortmanns, 1996)

$$\langle \mathcal{O} \rangle = \frac{1}{Z} \int \mathcal{D}A_\mu \mathcal{D}\bar{\psi} \mathcal{D}\psi \mathcal{O}(A_\mu, \bar{\psi}, \psi) \exp[-S(A_\mu, \bar{\psi}, \psi; g, m_i)], \quad (11.11)$$

where  $A_\mu$  denotes the gauge fields,  $\bar{\psi}, \psi$  stand for the particle fields (indices  $f = 1, \dots, N_f$  for the ‘flavors’ and  $c = 1, \dots, N_c$  for the ‘colors’ classifying these quarks we suppressed, to simplify the notation). The action functional  $S$  also contains the gauge coupling and the quark masses  $m_i$  as parameters, and is the space–time integral of the Lagrange density of QCD,

$$S = \int d\tau \int d\mathbf{x} \mathcal{L}_{\text{QCD}}(A_\mu, \bar{\psi}, \psi; g, m_i); \quad (11.12)$$

the explicit form of  $\mathcal{L}_{\text{QCD}}$  in full generality is rather complicated, but will not be needed here. Finally, the normalizing factor  $Z$  in Eqn. (11.11), the vacuum-to-vacuum amplitude, is

$$Z = \int \mathcal{D}A_\mu \mathcal{D}\psi \mathcal{D}\bar{\psi} \exp[-S]. \quad (11.13)$$

The formal analogy of Eqns. (11.11)–(11.13) with problems in statistical mechanics is rather obvious: if we interpret  $\mathcal{L}_{\text{QCD}}$  as a density of an effective free energy functional, multiplied by inverse temperature  $\beta$ , the action can be interpreted as effective Hamiltonian  $\beta\mathcal{H}$ , and  $Z$  is analogous to a partition function. Now it is already well known for the path integral formulation of simple non-relativistic quantum mechanics (Feynman and Hibbs, 1965) that a precise mathematical meaning must be given to all these functional integrals over gauge and matter fields. One very attractive way to do this is the

lattice formulation in which the  $(3 + 1)$ -dimensional space–time continuum is discretized on a hypercubic lattice. A gauge-invariant lattice action must be chosen, which then provides a gauge-invariant scheme to regularize the path integral: in the limit where the lattice linear dimensions become large, the continuum limit is recovered.

In practice such a lattice action can be chosen following Wilson (1974) associating matter variables  $\psi_x, \bar{\psi}_x$  with the sites of the lattice and gauge variables with the links,  $U_x^\mu$  being associated with a link leaving a site  $x$  in direction  $\hat{\mu}$ . These link variables are elements of the gauge group  $SU(N)$  and replace the continuum gauge fields  $A_\mu$ . One can then show that a gauge action that produces the correct continuum limit (namely  $(4g^2)^{-1} \int dt \int d\mathbf{x} \text{Tr} F_{\mu\nu}^2$  where  $F_{\mu\nu}$  is the Yang–Mills field strength) can be expressed in terms of products of these link variables over closed elementary plaquettes of the hypercubic lattice,

$$S = \frac{2N}{g^2} \sum_{\substack{x \\ \mu < \nu}} p_x^{\mu\nu}, \quad p_x^{\mu\nu} = 1 - \frac{1}{N} \text{Tr} U_x^\mu U_{x+\hat{\mu}}^\nu U_{x+\hat{\mu}}^{\mu+} U_x^{\nu+}, \quad (11.14)$$

where  $\text{Tr}$  denotes the trace in color space (normally  $N = 3$ , quarks exist in three colors, but corresponding studies using the  $SU(2)$  group are also made).

If one treats pure gauge fields, the problem closely resembles the treatment of spin problems in the lattice as encountered in previous chapters – the only difference being that  $\beta$  then corresponds to  $g^{-2}$ , and, rather than a bilinear Hamiltonian in terms of spins on lattice sites, one has to deal with a Hamiltonian containing those products of link variables around elementary plaquettes.

The problem becomes far more involved if the matter fields  $\psi(x), \bar{\psi}(x)$  describing the quarks are included: after all, quarks are fermions, and hence these fields really are operators obeying anticommutation rules (so-called Grassmann variables). There is no practical way to deal with such fermionic fields explicitly in the context of Monte Carlo simulations.

Fortunately, this aspect of QCD is somewhat simpler than the many-fermion problems encountered in condensed matter physics (such as the Hubbard Hamiltonian, etc., see Chapter 8): the Lagrangian of QCD contains  $\bar{\psi}$  and  $\psi$  only in bilinear form, and thus one can integrate out the matter fields exactly. The price that has to be paid is that a complicated determinant appears, which is very cumbersome to handle and requires special methods, which are beyond consideration here (Herrmann and Karsch, 1991). Thus, sometimes this determinant is simply ignored (i.e. set equal to unity), but this so-called ‘quenched approximation’ is clearly uncontrolled, although there is hope that the errors are relatively small.

What do we wish to achieve with this lattice formulation of QCD? One very fundamental problem that the theory should master is the prediction of the masses of the hadrons, using the quark mass as an input. Very promising results for the mass of the nucleon, the pion, the delta baryon, etc., have indeed

been obtained (Butler *et al.*, 1993), although the results are still to be considered somewhat preliminary due to the use of the ‘quenched approximation’ mentioned above.

There are many more problems in QCD where the analogy with problems encountered in condensed matter physics is even closer, namely phase transitions occurring in nuclear matter of very high energy (or in other words, at very high ‘temperature’: 100 MeV corresponds to  $1.16 \times 10^{12}$  K.) While the phase transitions in condensed matter physics occur at the scale from 1 K to  $10^3$  K, at  $T_c \approx (2.32 \pm 0.6) \times 10^{12}$  K one expects a ‘melting’ of nuclear matter – quarks and gluons cease to be confined inside hadrons and begin to move freely (Meyer-Ortmanns, 1996). According to the big bang theory of the early universe, this confinement transition should have happened at about  $10^{-6}$  sec after the big bang.

We now turn to some special aspects of the average in Eqn. (11.11). Due to the Wick rotation ( $it \rightarrow \tau$ ) inverse temperature appears as an integration limit of the  $\tau$  integration,

$$S = \int_0^\beta d\tau \int d\mathbf{x} \mathcal{L}(A_\mu, \bar{\psi}, \psi, g, m_i) \quad (11.15)$$

and in addition boundary conditions have to be obeyed,

$$A_\mu(\mathbf{x}, 0) = A_\mu(\mathbf{x}, \beta), \quad \psi(\mathbf{x}, 0) = -\psi(\mathbf{x}, \beta), \quad \bar{\psi}(\mathbf{x}, 0) = -\bar{\psi}(\mathbf{x}, \beta). \quad (11.16)$$

Thus, while one has periodic boundary conditions in pseudo-time direction for the gauge fields, as is familiar from condensed matter physics problems, the particle fields require antiperiodic boundary conditions. As we shall discuss in the next section, there is intense interest in understanding the order of this deconfinement transition, and the problems in its analysis have many parallels with studies of the Potts model in statistical mechanics.

## 11.7 THE DECONFINEMENT TRANSITION OF QCD

The deconfinement transition of a pure gauge model employing the SU(3) symmetry can be considered as the limit of QCD in which all quark masses tend to infinity. Real physics, of course, occurs at finite quark masses (remember that there exist two light quarks, called ‘up’ and ‘down’, and one heavier one, the so-called ‘strange quark’). This case is difficult to treat, and therefore another simplified limit of QCD has been considered, where the quark masses are put all equal to zero. This limit is called the ‘chiral limit’, because a Lagrange density applies which exhibits the so-called ‘chiral symmetry’ and is reminiscent of Landau theory, Eqn. (2.49), the central distinction being that the scalar order parameter field  $m(\mathbf{x})$  is now replaced by an  $N_f \times N_f$  matrix field  $\phi$  (Pisarski



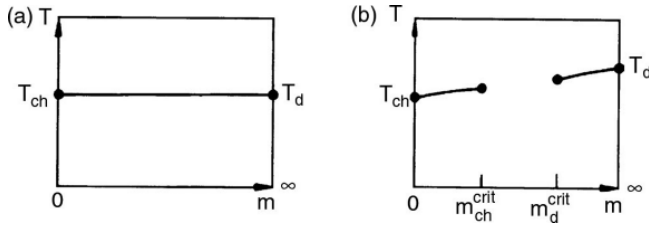


Fig. 11.3 Hypothetical phase diagrams of QCD in the  $(m, T)$  plane, where  $T$  is the temperature, and  $m$  stands for generic quark masses. (a) The transitions persist for finite non-zero  $m$  and coincide. (b) Both transitions terminate at critical points for intermediate mass values. After Meyer-Ortmanns (1996).

and Wilczek, 1984)

$$\mathcal{L} = \frac{1}{2} \text{Tr} \left( \frac{\partial \phi^+}{\partial x_\mu} \right) \left( \frac{\partial \phi}{\partial x_\mu} \right) - \frac{f}{2} \text{Tr}(\phi^+ \phi) - \frac{\pi^2}{3} [f_1 (\text{Tr} \phi^+ \phi)^2 + f_2 \text{Tr}(\phi^+ \phi)^2] + g(\det \phi + \det \phi^+). \quad (11.17)$$

Here  $f, f_1, f_2$ , and  $g$  are constants. At zero temperature there is a symmetry-broken state, i.e. the vacuum expectation value  $\langle \phi \rangle$  (which is also called the ‘quark condensate’) is non-zero but exhibits  $SU(N_f)$  symmetry. This spontaneous breaking of chiral symmetry is associated with the occurrence of a multiplet of Goldstone bosons (i.e. massless excitations, loosely analogous to spin wave excitations in a Heisenberg ferromagnet).

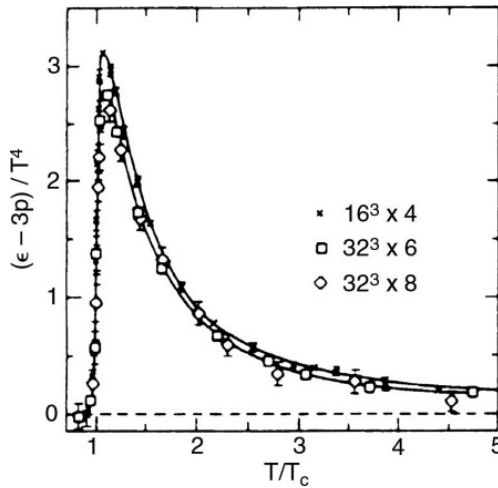
At finite temperature this model is believed to undergo a phase transition to a phase where the chiral symmetry is restored. One believes that for  $g$  of order unity this transition is of second order for  $N_f = 2$  but of first order for  $N_f = 3$ . The obvious problem is that QCD leads to rather different phase transitions in the limit of quark masses  $m \rightarrow \infty$  and  $m \rightarrow 0$ : Note that the order parameter for the deconfinement transition is rather subtle, namely the expectation value of a Wilson loop,  $\langle L(\mathbf{x}) \rangle$ , where  $L(\mathbf{x})$  is defined by

$$L(\mathbf{x}) \equiv \text{Tr} \hat{T} \exp \left( \int_0^\beta dt A_0(\mathbf{x}, t) \right), \quad (11.18)$$

where  $\hat{T}$  is the time-ordering operator. One can interpret  $\langle L(\mathbf{x}) \rangle$  in terms of the free energy  $F(\mathbf{x})$  of a free test quark inserted into the system at  $\mathbf{x}$ ,  $\langle L(\mathbf{x}) \rangle = \exp[-\beta F(\mathbf{x})]$  is zero in the phase exhibiting quark confinement, while  $\langle L(\mathbf{x}) \rangle$  is non-zero if we have deconfinement. This behavior qualifies  $\langle L(\mathbf{x}) \rangle$  as an order parameter of the deconfinement transition.

The question now is what happens when we consider intermediate quark masses: are the deconfinement transition at  $T_d$  and the chiral transition at  $T_{ch}$  simply limits of the same transition within QCD which smoothly changes its character when the quark masses are varied, or are these transitions unrelated to each other (and then ending at critical points somewhere in the  $(T, m)$  plane), Fig. 11.3? If scenario (b) applies and if the physically relevant quark masses

Fig. 11.4 Interaction measure  $\varepsilon - 3p$  normalized to  $T^4$  (dimensionless units) plotted vs.  $T/T_c$  for a pure SU(3) gauge theory for different lattice sizes. From Karsch (1995).



lie in the range in between  $m_{\text{ch}}^{\text{crit}} < m < m_{\text{d}}^{\text{crit}}$ , no phase transition occurs but rather the change of nuclear matter to the quark–gluon plasma is a gradual, smooth crossover (as the change of a gas of neutral atoms into a plasma of ions and electrons when the temperature of the gas is raised).

From Fig. 11.3 we recognize that a crucial problem of QCD is the clarification of a phase diagram (whether or not a sharp phase transition occurs, and if the answer is yes, what is the order of the transition). If there were a first order transition, this should have experimentally observable consequences for heavy-ion collisions. Also the abundance of light elements in the universe has been attributed to consequences of the first order scenario, but one must consider this idea rather as an unproven speculation.

Before one can address the behavior of QCD for intermediate quark masses, it clearly is of central importance to clarify the phase transitions in the two limiting cases of Fig. 11.3,  $m \rightarrow 0$  and  $m \rightarrow \infty$ . Even this problem has led to long-standing controversies, e.g. the order of the deconfinement transition ( $m \rightarrow \infty$ ) has been under debate for some time, but now the controversy seems to be settled (Meyer-Ortmanns, 1996) by the finding of a (relatively weak) first order transition. The equation of state  $\Delta = (\varepsilon - 3p)/T^4$  of a pure SU(3) gauge model is plotted in Fig. 11.4 (Karsch, 1995). Here  $\varepsilon$  is the energy density  $\{\varepsilon = -(1/V)\partial(\ln Z)/\partial(1/T)\}$  and  $p$  is the pressure  $\{p = T(\partial/\partial V)\ln Z\}$  of nuclear matter. These definitions are just the usual ones in the continuum limit, of course. In order to evaluate such derivatives in the framework of lattice gauge theory one has to introduce the lattice spacing for the ‘temporal’ direction ( $a_\tau$ ) and spatial directions ( $a_\sigma$ ) as explicit variables (the volume then is  $V = a_\sigma^3 N_\sigma^3 a_\tau N_\tau$  for a lattice of linear size  $N_\sigma$  in the spatial directions and  $N_\tau$  in the ‘time’ direction). Treating  $a_\tau$  and  $a_\sigma$  as continuous variables, one can write  $\partial/\partial T = N_\tau^{-1}\partial/\partial a_\tau$ , and  $\partial/\partial V = (3a_\sigma^2 N_\sigma^3)\partial/\partial a_\sigma$ . After performing the appropriate lattice derivatives of  $\ln Z$ , one can set the lattice spacings equal again,  $a_\sigma = a_\tau = a$ , and use  $a$  as the unit of length. However, when one wishes to extrapolate towards the continuum limit, one needs

to let  $N_\tau \rightarrow \infty$ ,  $a_\tau \rightarrow 0$  keeping the temperature  $(N_\tau a_\tau)^{-1} = T$  fixed at the physical scale of interest (MeV units). Therefore one needs to study the dependence of the data on  $N_\tau$  carefully, as shown in Fig. 11.4. A detailed analysis of the steep rise of  $\varepsilon - 3p$  at  $T_c$  shows that there indeed occurs a first order phase transition, with a latent heat of  $\Delta\varepsilon/T_c^4 = 2.44 \pm 0.24$  ( $N_\tau = 4$ ) or  $\Delta\varepsilon/T_c^4 = 1.80 \pm 0.18$  ( $N_\tau = 6$ ), respectively. An important conclusion from the equation of state as shown in Fig. 11.4 also is the fact that interaction effects are still present at temperatures far above  $T_c$  (for a non-interacting ideal gas one would have  $\varepsilon = 3p$ , of course).

Another quantity which has found much attention is the interface tension between low temperature and high temperature phases at the deconfinement transition, since this quantity plays a role in some of the scenarios that describe the evolution of the early universe. This interface tension was measured by Iwasaki *et al.* (1994) by an extension of the finite size analysis of distribution functions originally proposed for the Ising model (Binder, 1982). The result is  $\sigma/T_c^3 = 0.0292 \pm 0.0022$  for  $N_\tau = 4$  and  $\sigma/T_c^3 = 0.0218 \pm 0.0033$  for  $N_\tau = 6$ . Note that all these calculations are extremely time-consuming and difficult – early estimates for  $\sigma/T_c^3$  applying different methods ended up with estimates that were nearly an order of magnitude too large. For a description of the dynamics of the early universe, this interface tension controls the extent to which the quark–gluon plasma at the deconfinement transition could be supercooled, before hadrons are nucleated. For the estimates of  $\sigma/T_c^3$  quoted above, one ends up finally with the result that the average distance between hadronic bubbles should have been  $22 \pm 5$  nm (Meyer-Ortmanns, 1996).

## 11.8 TOWARDS QUANTITATIVE PREDICTIONS

Lattice QCD has continued to evolve because of improved models, new simulation methods and faster computers. Indeed this area is arguably the one in which reliance on special purpose computers is greatest. The last few years have seen a continued evolution away from the use of the quenched approximation to included dynamical fermions. The removal of this quenched constraint removes a barrier to more realistic estimates. System sizes as large as  $32 \times 32 \times 32 \times 100$  lattice spacings have been simulated, with the major computational roadblocks being critical slowing down and the inversion of the fermion propagator for small masses. A rather complete description of these advances can be found in the review by DeGrand (2004).

Lattice QCD can produce more precise data and treat smaller quark masses, so that it is now possible to make quantitative comparisons with experiment. There are now high quality Monte Carlo simulations available that include vacuum-polarization effects for three (dynamical) light quarks. Corrections were made for finite volume effects ( $\sim 1\%$ ) and finite lattice spacing effects ( $\sim 2\text{--}3\%$ ). Final ‘best’ estimates for nine different quantities are shown in Fig. 11.5. The determination was limited to a restricted set of (‘gold plated’)

Fig. 11.5 Ratio of lattice QCD estimates from Monte Carlo simulations for different quantities to the experimental values: (left) with vacuum polarization, (right) without vacuum polarization. From Davies *et al.* (2004).

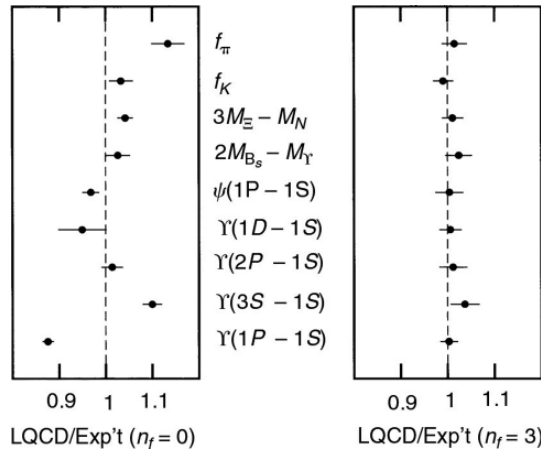
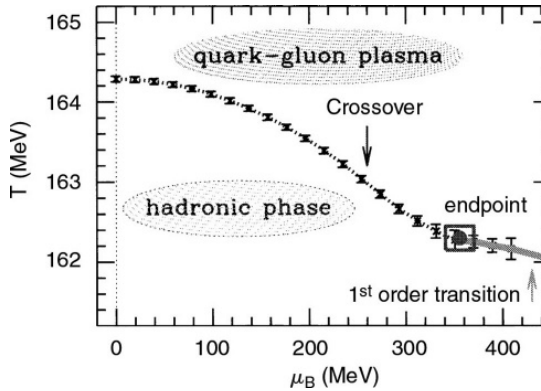


Fig. 11.6 Phase diagram for dynamical QCD obtained by using two-dimensional histogram reweighting of Monte Carlo data generated at  $\mu = 0$ . The small square shows the location of the endpoint to the line of first order transitions which is a critical point. From Fodor and Katz (2004).



parameters, but it nonetheless provides a good indication of the progress that was made.

Another relatively recent development is the use of Monte Carlo simulations to study QCD at finite density, i.e. to extend the simulations to non-zero baryonic chemical potential  $\mu$  (Fodor and Katz, 2002, 2004). This is not straightforward to do since the determinant of the Euclidean Dirac operator is complex and thus complex weights result for the probability that would be used for Monte Carlo sampling. (This is reminiscent of the ‘sign problem’ that was mentioned in Section 8.3.4 for quantum Monte Carlo studies.) The key to their approach was to perform Monte Carlo simulations for  $\mu = 0$  and then use two-dimensional histogram reweighting (see Section 7.2) to extrapolate to non-zero  $\mu$ . They found a first order phase boundary extending into the  $\mu - T$  plane and terminating at a critical point at  $\mu = 360(40)$  MeV and  $T = 162(2)$  MeV. This boundary is depicted in Fig. 11.6. Beyond the critical point there is only a rapid but non-singular change in properties so that there is no true transition between the hadronic phase and the quark-gluon plasma. (Alternatively, data could be generated for complex  $m$  and then attempt to

analytically continue the phase diagram to real chemical potential.) This is but one further example of how methods first applied in one sub-field of physics can be transferred successfully into another area.

Monte Carlo simulations of lattice QCD continue to be of great interest (Alexandrou *et al.*, 2006). A very thorough study of lattice QCD using the quenched approximation with light sea quarks by Dürr *et al.* (2008) has now been used successfully to calculate light hadron masses, i.e. to produce values that are in good quantitative agreement with experiment. Further study of finite temperature phase diagrams remains challenging in spite of the development of new techniques and the appearance of faster computers (Fodor, 2006). Avoiding chiral symmetry breaking remains an important goal that has been beyond the reach of past generations of supercomputers. To a great extent chiral symmetry can be restored using ‘domain wall fermions’ through the introduction of a fifth dimension, but the computational needs are so great that it will only be possible to reduce the effects of symmetry breaking to a minimal amount using a lattice QCD code (LQCD) on petaflop machines (Luu *et al.*, 2007). We note in passing that the LQCD code just mentioned runs with almost perfect speedup all the way up to 131 072 processors on the Blue Gene/L supercomputer. It should then be possible to determine the equation of state of the quark–gluon plasma just as protons and neutrons began to form in the early universe.

As one example of the progress that has been made in recent years, we refer the reader to a nice study of  $2 + 1$  flavor lattice QCD by Aoki *et al.* (2010). Here, a multi-author collaboration used a sophisticated, hybrid Monte Carlo algorithm on a  $32^3 \times 64$  lattice together with single histogram reweighting techniques (see Section 7.2) to extract estimates for hadron and quark masses as well as the pseudo-scalar decay constants on the physical point. For a good overview of the ‘state-of-the-art’ in this field we refer the interested reader to a recent review by Fodor and Hoelbling (2012).

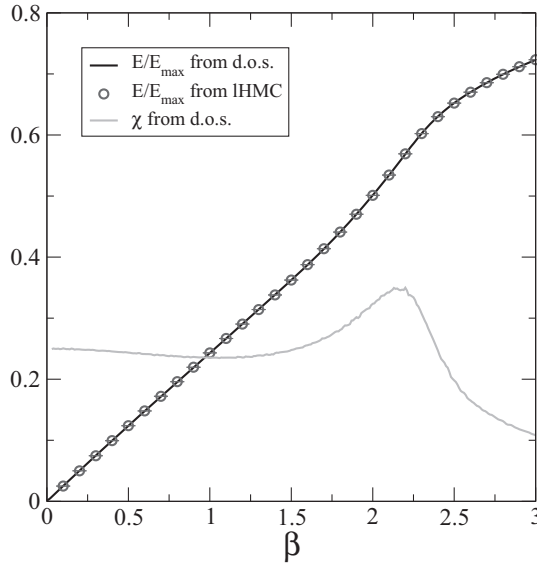
### 11.9 DENSITY OF STATES IN GAUGE THEORIES

The determination of observables in lattice gauge theories that cannot be expressed as a vacuum expectation value is inefficient by standard Monte Carlo methods. Instead, Langfeld *et al.* (2012) adapted Wang–Landau sampling (see Section 7.8) to determine the density of states  $g(E)$  for lattice gauge theories. They approximate  $\ln g(e)$  by a piecewise linear function

$$g(E) = g(E_0) \exp\{a(E_0)(E - E_0)\}. \quad (11.19)$$

Using an iterative method they estimate the value for  $a(E_0)$  and then put all the pieces together to obtain the full density of states that can then be used to calculate observables. This approach was successfully applied to  $U(1)$ ,  $SU(2)$ , and  $SU(3)$  gauge theories. For  $SU(2)$  gauge theory, results were obtained for the density of states over 120 000 orders of magnitude for a  $20^4$  system. The

Fig. 11.7 Average plaquette vs. inverse coupling  $\beta$  for a SU(2) lattice gauge theory on a  $10^4$  lattice obtained from a density of states estimate and from a localized hybrid Monte Carlo (LHMC) simulation. Also shown is the specific heat  $\chi(\beta) = (\langle E^2 \rangle - \langle E \rangle^2) / 6L^4$ . After Langfeld *et al.* (2012).



algorithm was carefully checked, and in Fig. 11.7 the comparison of results for the plaquette versus inverse coupling  $\beta$  obtained from the density of states and with a localized hybrid Monte Carlo algorithm for SU(2) gauge theory on a  $10^4$  lattice shows excellent agreement.

## 11.10 PERSPECTIVE

Of course, this brief introduction was not intended to give a representative coverage of the extensive literature on Monte Carlo applications in lattice gauge theory; we only want to give the reader a feeling for the ideas underlying the approach and to make the connections with Monte Carlo applications in the statistical mechanics of condensed matter transparent.

Because of the magnitude of the computer resources that are needed to make progress in this field, Monte Carlo simulations of lattice gauge models will continue to provide a testing ground for the efficient use of petaflop and exaflop machines of the future.

## REFERENCES

- |                                                                                                                                                                                                                                                                               |                                                                                                                                                                                                                                                                |
|-------------------------------------------------------------------------------------------------------------------------------------------------------------------------------------------------------------------------------------------------------------------------------|----------------------------------------------------------------------------------------------------------------------------------------------------------------------------------------------------------------------------------------------------------------|
| <p>Alexandrou, C., de Forcrand, P., and Lucini, B. (2006), <i>Phys. Rev. Lett.</i> <b>97</b>, 222002.</p> <p>Aoki, S. <i>et al.</i> (PACS-CS Collaboration) (2010), <i>Phys. Rev. D</i> <b>81</b>, 074503.</p> <p>Binder, K. (1982), <i>Phys. Rev. A</i> <b>25</b>, 1699.</p> | <p>Bock, W., Evertz, H. G., Jersak, J., Landau, D. P., Neuhaus, T., and Xu, J. L. (1990), <i>Phys. Rev. D</i> <b>41</b>, 2573.</p> <p>Butler, F., Chen, H., Sexton, J., Vaccarino, A., and Weingarten, D. (1993), <i>Phys. Rev. Lett.</i> <b>70</b>, 7849.</p> |
|-------------------------------------------------------------------------------------------------------------------------------------------------------------------------------------------------------------------------------------------------------------------------------|----------------------------------------------------------------------------------------------------------------------------------------------------------------------------------------------------------------------------------------------------------------|

- Creutz, M., Jacobs, L., and Rebbi, C. (1979), *Phys. Rev. Lett.* **42**, 1390.
- Creutz, M., Jacobs, L., and Rebbi, C. (1983), *Phys. Rep.* **93**, 207.
- Davies, C. T. H., Follana, E., Gray, A., Lepage, G. P., Mason, Q., Nobes, M., Shigemitsu, J., Aubin, C., Bernard, C., Burch, T., DeTar, C., Gottlieb, S., Gregory, E. B., Heller, U. M., Hetrick, J. E., Osborn, J., Sugar, R., Toussaint, D., Di Pierro, M., El-Khadra, A., Kronfeld, A. S., Mackenzie, P. B., Menscher, D., and Simone, J. (2004), *Phys. Rev. Lett.* **92**, 022001.
- DeGrand, T. (2004), *Int. J. Mod. Phys. A* **19**, 1337.
- Dürr, S., Fodor, Z., Frison, J., Hoelbling, C., Hoffmann, R., Katz, S. D., Krieg, S., Kurth, T., Lellouch, L., Lippert, T., Szabo, K. K., and Vulvert, G. (2008), *Science* **32** (2), 1224.
- Feynman, R. P. and Hibbs, A. R. (1965), *Quantum Mechanics and Path Integrals* (McGraw-Hill, New York).
- Fodor, Z. (2006), *Nucl. Phys. B* (Proc. Suppl.) **153**, 98.
- Fodor, Z. and Hoelbling, C. (2012), *Rev. Mod. Phys.* **84**, 449.
- Fodor, Z. and Katz, S. D. (2002), *JHEP* **0203**, 014.
- Fodor, Z. and Katz, S. D. (2004), *JHEP* **0404**, 050.
- Herrmann, H. J. and Karsch, F. (1991), *Fermion Algorithms* (World Scientific, Singapore).
- Iwasaki, Y., Kanaya, K., Karkkainen, L., Rummukainen, K., and Yoshie, T. (1994), *Phys. Rev. D* **49**, 3540.
- Jersák, J., Lang, C. B., and Neuhaus, T. (1996a), *Phys. Rev. Lett.* **77**, 1933.
- Jersák, J., Lang, C. B., and Neuhaus, T. (1996b), *Phys. Rev. D* **54**, 6909.
- Karsch, F. (1995), *Nucl. Phys. A* **590**, 367.
- Kogut, J. B. (1983), *Rev. Mod. Phys.* **55**, 775.
- Langfeld, K., Lucini, B., and Rago, A. (2012), *Phys. Rev. Lett.* **109**, 111601.
- Luu, T., Soltz, R., and Vranos, P. (2007), *Comput. Sci. Eng.* **9**, 55.
- Meyer-Ortmanns, H. (1996), *Rev. Mod. Phys.* **68**, 473.
- Montvay, I. and Münster, G. (1994), *Quantum Fields on the Lattice* (Cambridge University Press, Cambridge).
- Pisarski, R. D. and Wilczek, F. (1984), *Phys. Rev. D* **29**, 338.
- Wansleben, S. and Zittartz, J. (1987), *Nuclear Phys. B* **280**, 108.
- Wilson, K. (1974), *Phys. Rev. D* **10**, 2455.